

Development of fluorescent- and radio-traceable T1307-polymeric micelles as biomedical agents for cancer diagnosis: biodistribution on 4T1 tumor-bearing mice

Nicole Lecot^{1,*}, Gonzalo Rodríguez², Valentina Stancov², Marcelo Fernández³, Mercedes González², Romina J. Glisoni⁴, Pablo Cabral⁵, Hugo Cerecetto^{2,5,*}

¹Laboratorio de Técnicas Nucleares Aplicadas a Bioquímica y Biotecnología, Centro de Investigaciones Nucleares, Facultad de Ciencias, Universidad de la República, Uruguay, ²Grupo de Química Orgánica Medicinal, Instituto de Química Biológica, Facultad de Ciencias, Universidad de la República, Uruguay, ³Laboratorio de Experimentación Animal, Centro de Investigaciones Nucleares, Facultad de Ciencias, Universidad de la República, Uruguay, ⁴Departamento de Tecnología Farmacéutica, Cátedra de Tecnología Farmacéutica II, CONICET-Instituto de Nanobiotecnología (NANOBIOTEC), Facultad de Farmacia y Bioquímica, Universidad de Buenos Aires, Argentina, ⁵Área de Radiofarmacia, Centro de Investigaciones Nucleares, Facultad de Ciencias, Universidad de la República, Uruguay

In recent years, nanocarriers have been studied as promising pharmaceutical tools for controlled drug-delivery, treatment-efficacy follow-up and disease imaging. Among them, X-shaped amphiphilic polymeric micelles (Tetronic®, poloxamines) display great potential due to their biocompatibility and non-toxic effects, among others. In the present work, polymeric micelles based on the T1307 copolymer were initially decorated with a 4,4-difluoro-4-bora-3a,4a-diazas-indacene (BODIPY)-fluorophore in order to determinate its *in vivo* biodistribution on 4T1 tumor-bearing mice. However, unfavorable results with this probe led to two different strategies. On the one hand, the BODIPY-loaded micelles, **L-T1307-BODIPY**, and on the other hand, the ^{99m}Tc-radiolabeled micelles, **L-T1307-^{99m}Tc**, were analyzed separately *in vivo*. The results indicated that T1307 accumulates mainly in the stomach, the kidneys, the lungs and the tumor, reaching the maximum organ-accumulation 2 hours after intravenous injection. Additionally, and according to the results obtained for **L-T1307-^{99m}Tc**, the capture of the polymeric micelles in organs could be observed up to 24 hours after injection. The results obtained in this work were promising towards the development of new radiotracer agents for breast cancer based on X-shaped polymeric micelles.

Keywords: Amphiphilic polymeric micelles. T1307. BODIPY. ^{99m}Tc. *In vivo* biodistribution. Cancer diagnosis.

INTRODUCTION

Cancer is the second leading cause of death in the world. Among the different types of cancer are the solid tumors, i.e., carcinomas, sarcomas and lymphomas. In this sense, nanotechnology has been growing very fast in

terms of developing new strategies against solid tumors, by optimizing diagnostic efficiency, developing novel anticancer treatments, and reducing the toxicity and improving the aqueous solubility of the drug candidates (Glisoni, Sosnik, 2014a; Lv *et al.*, 2013; Glisoni *et al.*, 2013; Glisoni *et al.*, 2012). The use of nanotechnology is purportedly related to the enhanced permeability and retention effect (EPR), which takes advantage of the properties of solid tumors that may promote angiogenesis and ensure high blood supply to the growing mass, causing imperfect vascular structures and a significant

*Correspondence: H. Cerecetto. N. Lecot. Centro de Investigaciones Nucleares. Facultad de Ciencias. Universidad de la República. Mataojo 2055. 11400 Montevideo, Uruguay. E-mails: hcerecetto@cin.edu.uy; nlecot@cin.edu.uy. ORCID: 0000-0003-1256-3786 (Hugo Cerecetto) 0000-0003-2531-8026 (Nicole Lecot)

lack of lymphatic drainage. The EPR could allow the extravasation of nanomaterials and their accumulation inside the pathological site (Eawsakul *et al.*, 2017; Maeda *et al.*, 2000).

Nanomedicines allow early tumor diagnosis, which is the most important fact to increase patient survival (Oda *et al.*, 2017). Several types of nanosystems for diagnostic imaging have been described; among them, quantum dots, gold nanoparticles, carbon nanotubes, silica nanoparticles, liposomes, nano micelles and dendrimers can be highlighted (Acharya, Mitra, Cholkar, 2017). These nanosystems have the following advantages, among others: *i*) their nanometrical size, *ii*) the possibility of surface functionalization for active drug-delivery, *iii*) their passive targeting, *iv*) the solubilization of poorly soluble molecules in aqueous milieu, *v*) the protection of encapsulated substances from degradation and metabolism, *vi*) improved pharmacokinetic effects. These nanodevices particularly used in diagnostic imaging have been described coupled with magnetic resonance, optical, nuclear, computed tomography and ultrasound imaging (Acharya, Mitra, Cholkar, 2017; Marques Grallert *et al.*, 2012). Advanced thermosensitive nanomaterials are promising “smart materials” for diagnosis when stimulated at a particular temperature range (Nardeccchia *et al.*, 2019; Cohn, Sosnik, Levy, 2003).

Among the different nanosystems used in pharmaceutical formulations for diagnosis, due emphasis should be given to polymeric micelles (PMs) (Oda *et al.*, 2017; Mi *et al.*, 2013; Marques Grallert *et al.*, 2012), which are colloidal particles formed by the spontaneous self-assembly of amphiphilic moieties in water or by a solvent evaporation and rehydration method (Glisoni, Sosnik, 2014a; Oda *et al.*, 2017). Particularly, the X-shaped amphiphilic block copolymers (poloxamine, Tetronic®), with an ethylenediamine central group bonded to four arms of poly(propyleneoxide)-poly(ethyleneoxide) (PPO-PEO) blocks, display great potential as smart delivery systems, with modified biodistribution properties (Glisoni, Sosnik, 2014a; Glisoni, Sosnik, 2014b; Cuestas *et al.*, 2013; Marques Grallert *et al.*, 2012). The presence of the tertiary amines in the central chain cause this material to exhibit temperature and pH responsiveness (Glisoni, Sosnik, 2014a; Glisoni, Sosnik, 2014b;

Cuestas *et al.*, 2013). In particular, the T1307 copolymer (molecular weight 18,000 g mol⁻¹), which contains a large chain of PPO (mean number of propyleneoxide units per PPO block of 23) and another of PEO (mean number of ethyleneoxide units per PEO block of 72), forms physically stable PMs toward dilution and has been proposed as a drug-solubilizing nanocarrier, among other applications (González-López *et al.*, 2008; Chiappetta, Sosnik, 2007; Cohn *et al.*, 2003). Several studies have been performed to analyze the biodistribution of PMs *in vitro* and *in vivo* (Moghimi, Hunter, 2000; Araujo *et al.*, 1999; Töster, Müller, Kreuter, 1990), although a specific report on the *in vivo* biodistribution of T1307 PMs has not been found.

Considering this background, the purpose of our study was the development of T1307 PMs as nanocarriers for forthcoming *in vivo* studies as diagnostic agents. To this end, we studied the biodistribution of tumor-bearing mice, using two T1307-probes: *(i)* fluorescent- and *(ii)* radioactive-labeled.

MATERIAL AND METHODS

Material

Formyl-BODIPY and phosphonium ylide were prepared following previous descriptions (Wube *et al.*, 2011; Jiao *et al.*, 2009). Tetronic® 1307 (T1307; molecular weight 18,000 g mol⁻¹; PEO content 70 wt%) was donated by BASF Corporation (Buenos Aires, Argentina) and used as received. Triethylamine, *n*-hexane, methylenedichloride, CDCl₃, anhydrous dimethylformamide, tin (II) 2-ethylhexanoate (Sn(Oct)₂, 95%), D₂O, phosphate buffer saline (PBS), SnF₂·2H₂O, ethanol, saline, pyridine and acetic acid were all purchased from Sigma-Aldrich (St. Louis, MO, USA). Fetal bovine serum (FBS) and RPMI milieu were purchased from Capricorn Scientific (Germany). Solvents were dried over CaH₂ and stored over molecular sieve (4 Å). Other compounds were used without any purification process. Water was purified and deionized (18 MΩ/cm²) on a Milli-Q water filtration system (Millipore Corp., Milford, MA, USA). ⁹⁹Mo-^{99m}Tc generators were purchased from TecnoNuclear (Argentina).

Equipments

Fourier-transform infrared (FTIR) spectra were acquired, in solid state (KBr), using an IR-Prestige21 FTIR-ATR infrared spectrophotometer (Shimadzu, Kyoto, Japan) with Happ-Genzel apodization. The analyzed region was in the range between 4000-400 cm^{-1} (10 scans, spectral resolution of 4 cm^{-1}). The solid lyophilized samples (**T1307-BODIPY**, **L-T1307-BODIPY** and lyophilized pristine T1307) were mounted on the ATR metal-glass plate and the spectra were obtained with the IR SOLUTION spectrum software, which were subsequently processed using Origin 8.

Nuclear Magnetic Resonance (NMR) spectra were performed in a Bruker DPX-400 spectrometer, operating at a frequency of 400.13 MHz for ^1H and 100.77 for ^{13}C . The NMR spectra were analyzed in 15 % w/v CDCl_3 solutions for **BODIPY-ester** and **T1307-BODIPY** ($n=2$), and in 15 % w/v $\text{DMSO}-d_6$ solutions for **L-T1307-BODIPY** ($n=3$). The spectra were obtained using the MestReNova 8.0 software.

Fluorescence spectra were performed in a microplate reader (Thermo Scientific™ Varioskan™ LUX multimode microplate reader, USA).

Particle size and zeta potential of **L-T1307-BODIPY** micelles were obtained from five repeated measurements by a dynamic laser-diffraction particle-size detector and a Malvern Zeta analyzer (Nano-ZS, Malvern Instruments, Malvern, UK), respectively. The measuring process was kept at 25 °C.

Radioactivity was counted in a CRC7 Capintec dose calibrator and in a solid scintillation counter detector with 3"×3" NaI(Tl) crystal associated with a single channel analyzer (ORTEC, Oak Ridge, TN).

The encapsulation efficiency (%EE) was determined by reverse-phase HPLC chromatography (RP-HPLC) (Agilent 1200 Series Infinity Star, Santa Clara, USA) with a 5 μm C-18 Kinetex column (Phenomenex) run with an aqueous solution of trifluoroacetic acid 0.05 % (solvent A) and ethyl acetate/trifluoroacetic acid 0.1 % (solvent B), at a flow rate of 1 mL/min and performed in a gradient of A:B (100:0) for 15 minutes, A:B (0:100) for 2 minutes and finally A:B (100:0) 3 minutes, with UV detection.

Animals

Balb/c female mice weighing 18-20 g were produced and provided by Unidad de Reactivos para Biomodelos de Experimentacion (URBE), Facultad de Medicina, Universidad de la República, Uruguay. The authors state that they followed the principles outlined in the Declaration of Helsinki for all animal experimental investigations. Animals were housed in wire mesh cages at 20 ± 2 °C with 12 h artificial light-dark cycles. The animals were fed *ad libitum* to standard pellet diet and water and were used after a minimum of 3 days acclimation to the housing conditions.

All protocols for animal experimentation were carried out in accordance with procedures authorized by the Ethical Committee for Animal Experimentation, Uruguay, by whom this project was previously approved (CHEA-UdelaR Protocol number 240011-001547-16).

Data analysis

The statistical analysis was performed using the Student's *t*-test (in a comparison between two groups); *p* level less or equal to 0.05 was defined to determine statistically significant differences.

Methods

Synthesis of the **T1307-BODIPY**

The synthesis of **T1307-BODIPY** followed a two-step reaction (Figure 1): synthesis of **BODIPY-ester** and conjugation of T1307 with **BODIPY-ester** to form **T1307-BODIPY**.

Synthesis of the **BODIPY-ester**

A mixture of **formyl-BODIPY** (80 mg, 0.28 mmol), **phosphonium ylide** (192 mg, 0.55 mmol) and triethylamine (69 μL) was stirred at room temperature during three days under a nitrogen atmosphere. The mixture was evaporated *in vacuo* and the product was isolated using a preparative thin layer chromatography (SiO_2 , *n*-hexane:methylenedichloride (9:1)). Red solid,

40 mg (40 %); $^1\text{H NMR}$ (CDCl_3 , 400 MHz) δ (ppm): 1.30 (3H, t), 2.34 (3H, s), 2.39 (3H, s), 2.46 (3H, s), 2.52

(3H, s), 2.56 (3H, s), 4.19 (2H, q), 6.01 (1H, d), 6.05 (1H, s), 7.60 (1H, d); $\lambda_{\text{excitation}}/\lambda_{\text{emission}}$ (DMSO) = 514/550 nm.

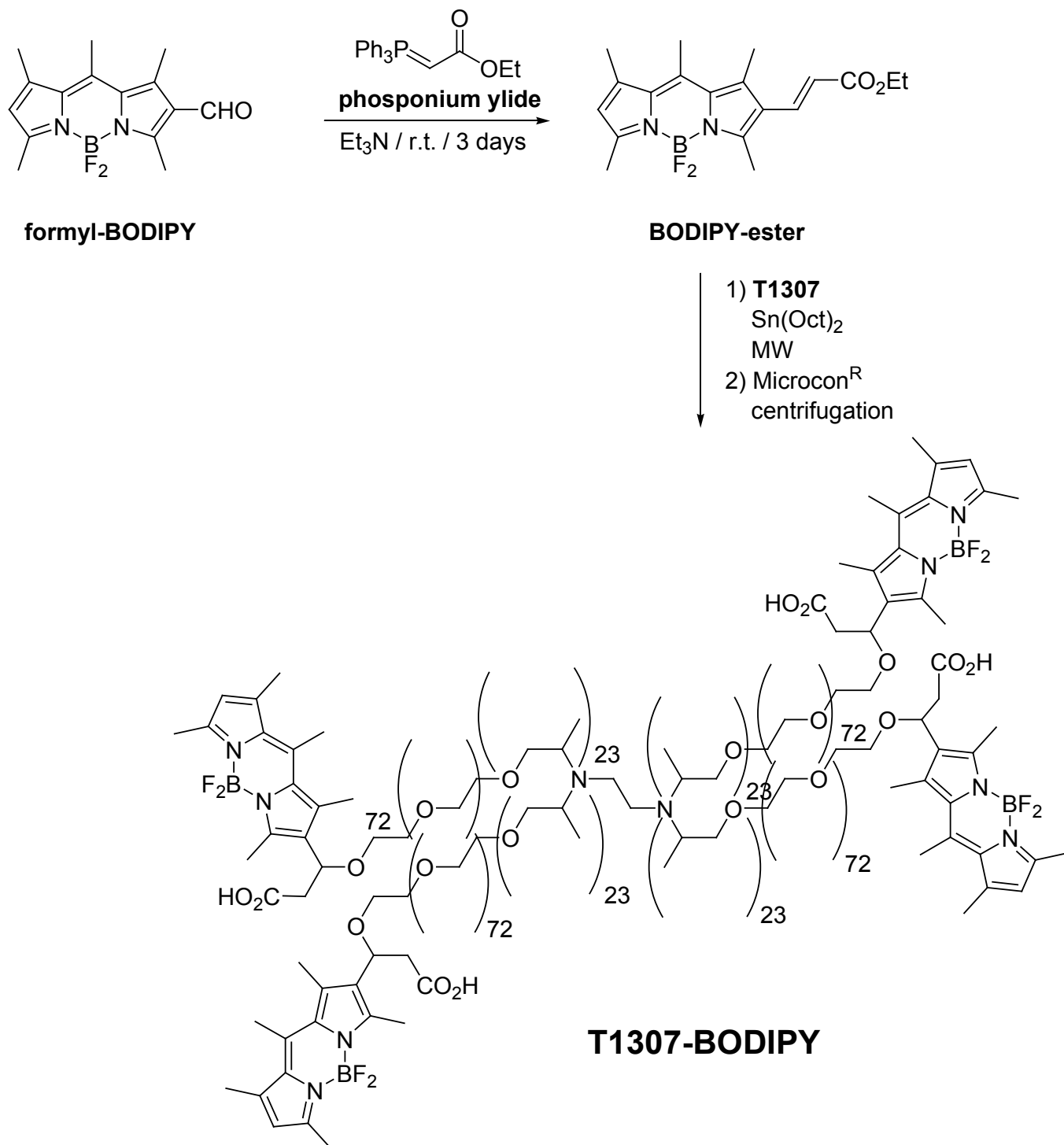


FIGURE 1 – Synthetic procedure for **T1307-BODIPY** obtention.

Synthesis of the T1307-BODIPY (Glisoni, Sosnik, 2014b)

T1307 (35 mg, 1.9 μmol) and **BODIPY-ester** (3 mg, 8.3 μmol) were dissolved in anhydrous dimethylformamide (2.6 mL). $\text{Sn}(\text{Oct})_2$ (0.63 μL) was added and the flask was placed in a microwave oven (multimode WX-4000, EU Chemical Instrument Co., with 20 mL Teflon reactors). The reaction mixture was exposed to the following microwave irradiation protocol: (i) two cycles of 5 minutes at 90 W power and (ii) one cycle of 5 minutes at 200 W power. The total reaction time was 15 minutes. The crude reaction solution was transferred to a Microcon® centrifugal filter (10 kDa) with a low-binding Ultracel® membrane. Centrifugation was performed at 12,000 rpm for 10 minutes. After that, the supernatant was eliminated and centrifuged at 5,000 rpm for 10 minutes. The resulting supernatant was again eliminated and the residue was washed with dimethylformamide (100 μL) and centrifuged at 3,500 g for 10 minutes. Finally, two cycles of washing with Milli-Q water (100 μL , each) and centrifugation at 3,500 g for 10 minutes were performed. The residue, which corresponds to the product, was dissolved in Milli-Q water and stored at $-20\text{ }^\circ\text{C}$ until it was used. ^1H NMR (CDCl_3 , 400 MHz) δ (ppm): 1.14 (276H, m, T1307- CH_3), 2.23-2.36 (12H, m, T1307-N $\text{CH}_2\text{CH}_2\text{N}$ - + 4 - $\text{CH}_2\text{CO}_2\text{H}$), 2.45 (12H, s, 4 BODIPY- CH_3), 2.51 (12H, s, 4 BODIPY- CH_3), 2.55 (12H, s, 4 BODIPY- CH_3), 2.66 (24H, s, 8 BODIPY- CH_3), 3.34-3.90 (1448H, m, T1307- CH_2 , T1307- CH and 4 BODIPY- $\text{CHCH}_2\text{CO}_2\text{H}$), 6.08-6.15 (4H, 3s, H-pyrrole); ^{13}C (from ^{13}C NMR, HSQC, and HMBC experiments, CDCl_3) δ (ppm): 5.0 (- CH_3), 12.6 (- CH_3), 14.0 (- CH_3), 21.5 (- CH_3), 36.0 (- $\text{CH}_2\text{CO}_2\text{H}$), 42.6 (- CH_2N), 70.6 (- CH_2O), 120.3, 127.9, 148.3, 149.0, 152.1, 165.9 (C=C and C=N), 170.9 (- CO_2H); IR (ν , cm^{-1}): 3443, 2913, 1656, 1103; $\lambda_{\text{excitation}}/\lambda_{\text{emission}}$ (PBS) = 514/550 nm.

Loading of T1307 with the fluorescent probe (**L-T1307-BODIPY**)

The typical encapsulation process was developed as follows: pristine **T1307** (50 mg) was hydrated in PBS (0.4 mL) and kept at $4\text{ }^\circ\text{C}$ for 30 minutes, after which the PBS was adjusted to a final volume of 0.5 mL and **BODIPY-ester** (2.9 mg) was added, followed by 1 h of stirring at room temperature. To remove the un-encapsulated fluorescent probe, it was centrifuged using

a Microcon® centrifugal filter (cut off 10 kDa) with the low-binding membrane of the mixture at 12,000 rpm for 10 minutes. Micelles were lyophilized and stored at $4\text{ }^\circ\text{C}$. The **L-T1307-BODIPY** was resuspended in MilliQ water and filtered by $0.22\text{ }\mu\text{M}$ for further studies (pH = 6.2). The encapsulation efficiency (%EE) was 82.7 %, particle size was 243 nm, polydispersity index was 0.32, and zeta potential was $-2.9 \pm 0.32\text{ mV}$. ^1H NMR ($\text{DMSO}-d_6$, 400 MHz) δ (ppm): 0.87 (3H, m, - $\text{CO}_2\text{CH}_2\text{CH}_3$), 1.00-1.30 (170H, m, T1307- CH_3), 2.30 (2.5H, m, T1307-N $\text{CH}_2\text{CH}_2\text{N}$ -), 2.46 (3H, s, BODIPY- CH_3), 2.56 (3H, s, BODIPY- CH_3), 2.70 (3H, s, BODIPY- CH_3), 4.19 (2H, q, - $\text{CO}_2\text{CH}_2\text{CH}_3$), 3.30-3.90 (890H, m, T1307- CH_2 and T1307- CH), 4.64 (2.5H, bs, OH), 6.12 (1H, d, - $\text{CH}=\text{CHCO}_2$ -), 6.37 (1H, s, H-pyrrole), 7.62 (1H, d, - $\text{CH}=\text{CHCO}_2$ -); IR (ν , cm^{-1}): 3432, 2965, 1770, 1155.

Loading of T1307 with the radioactive probe (**L-T1307- $^{99\text{m}}\text{Tc}$**) (García et al., 2018; Fernández et al., 2015; Giglio et al., 2008)

In order to label **T1307** directly by stannous reduction of $^{99\text{m}}\text{TcO}_4^-$, $\text{SnF}_2 \cdot 2\text{H}_2\text{O}$ (0.2 mL of stock ethanolic solution, 1 mg/mL) was added to a solution of **T1307** (0.5 mL of Milli-Q water, 0.15 g/mL) and $\text{Na}^{99\text{m}}\text{TcO}_4$ (14 mCi). The pH was then adjusted to 6.5. The mixture was incubated at room temperature for 20 minutes, then transferred to a Microcon® centrifugal filter (cut off 10 kDa) with the low-binding Ultracel® membrane, and centrifuged at 12,000 rpm for 10 minutes. The collected aqueous supernatant was used to determine the labeling yield, radiochemical purity (RP) and for further studies in animals (pH = 6.9). The labeling yield and RP were estimated by i) an ascending instant thin layer chromatography (ITLC) using the chromatographic systems: a) saline; b) pyridine:acetic acid:water (3:5:1.5 v/v), and ii) RP-HPLC using the conditions indicated above with UV and gamma detections. RP: 91.9 %.

Cell lines and culture conditions

The murine metastatic breast tumor cell line 4T1 (CRL-2539TM, ATCC®) was cultured in completed RPMI milieu supplemented with 10 % FBS. The culture was

grown in a humidified incubator containing 5 % CO₂ and maintained at 37 °C. The cells were centrifuged at 1,000 rpm for 5 minutes. The supernatant was removed and the pellet was resuspended in RPMI.

In vivo studies

Tumoral model (Dávila et al., 2019; Gao et al., 2016)

Cell suspensions were prepared at 7×10^6 cells/mL in RPMI milieu. Afterwards, five-six week old Balb/c female mice were inoculated subcutaneously (after the preparation of cell suspension) into the fourth inguinal mammary fat pad (100 µL/mouse). Animals were palpated daily in order to record the presence, location, and volume of all tumors. Tumor diameters were measured daily with a sterile caliper, calculated using the ellipsoidal method volume. Palpable tumors (~ 100 mm³) developed 5 days after the cell inoculation. Tumor diameters were measured daily with a vernier caliper (Ostrand-Rosenberg). The two diameters of the tumor, long (L) and short (C), were perpendicular to each other and covered the largest portion of the tumor in each direction. Tumor volume (V) was calculated using the following equation: $V = (C^2 \times L)/2$ (Chiang *et al.*, 2014; Dávila *et al.*, 2019).

In vivo and ex vivo fluorescence imaging of L-T1307-BODIPY on Balb/c mice with primary mammary tumors induced with 4T1 cells (Calzada et al., 2017)

At day 14 after the cell inoculation, fluorescence imaging study was conducted on Balb/c mice with induced 4T1 tumors by the intravenous injection (IV) of 50 mg of **L-T1307-BODIPY** per kg of body weight, via the animals' tails. For these experiments, the animals were anesthetized with isoflurane immediately before the injections. After being introduced into an optical imaging platform (In-Vivo MS FX PRO instrument, Bruker, Billerica, USA), the animals were measured using the X-ray and fluorescence modes (10 seconds acquisition, at excitation and emission wavelengths of 480 nm and 535 nm), 1 and 24 hours after the IV injections, n=3 for each time point. After each imaging time point, mice were sacrificed for organ dissection, macroscopic examination,

biodistribution and ex vivo imaging was carried out separately using the aforementioned imaging equipment. Animals without injection were used as negative control.

Biodistribution assay of L-T1307-99mTc on Balb/c mice with primary mammary tumors induced with 4T1 cells

Biodistribution study of the radioactive probe was performed by IV injections, via tail, of 856 µCi of the **L-T1307-^{99m}Tc** on Balb/c mice with and without 4T1-induced tumors (day 14 after cell inoculation). The animals, n=3 for each time point, were sacrificed by cervical dislocation 1, 2, 4 and 24 hours after the IV injections. The radioactivity in organs and tissues was measured in the solid scintillation counter detector described above. Organ weight correction was applied. The results are expressed as the percentage uptake of injected dose per tissue weight (%Act/g).

RESULTS AND DISCUSSION

Preparation and physicochemical characterization of fluorescent T1307-BODIPY and L-T1307-BODIPY probes

In order to generate a physiologically stable T1307-probe, we initially proposed the covalent conjugation between this copolymer and an adequate BODIPY-derivative (Rodríguez *et al.*, 2017). For that reason, we planned to use an ester containing BODIPY, i.e., **BODIPY-ester** (Figure 1), that could be able to react with the free-hydroxyl groups of the T1307 copolymer, via a conventional transesterification process in the presence of Sn(Oct)₂ as catalyst (Glisoni, Sosnik, 2014b). In this sense, a T1307 decorated with BODIPY moieties (**T1307-BODIPY**, Figure 1) was successfully prepared, through an assisted-microwave procedure, but ¹H NMR, ¹³C NMR, and IR spectroscopies suggested that the final product was the result of hydroxyl-1,4-addition followed by ester-hydrolysis, incorporating four units of BODIPY for each unit of T1307 (Figure 2B and 3). The **T1307-BODIPY** fluorescent probe had the same emission spectrum as the **BODIPY-ester** but did not show the same fluorescence intensity (Figure 4). Moreover, it displayed very poor

aqueous solubility (in PBS and PBS with up to 10 % of DMSO) and the aqueous solution had acidic pH (5.8). For this reason, all our attempts to carry out *in vivo* studies were unsuccessful.

Studies with fluorescent probe-loaded T1307 PMs (L-T1307-BODIPY)

BODIPY-ester loaded within **T1307** PMs was successfully performed in a short time, producing **L-T1307-BODIPY** with a %EE of 82.7 and nanometric size. The NMR and IR spectra of **L-T1307-BODIPY** confirmed a correct encapsulation process without structure modification of the **BODIPY-ester** fluorophore (compare Figures 2A and 2C, and see Figure 3).

After the IV injection of **L-T1307-BODIPY**, mice did not reveal toxicity effects on during *in vivo* studies, according to the Irwin test (Dávila *et al.*, 2019). This test

allowed us to consider the qualitative effects of **L-T1307-BODIPY** on behavior and physiological function, in the first dose that has observable effects as well as in doses that not induce behavioral toxicity.

It was possible to observe an accumulation of BODIPY-fluorophore in the region of the tumor after 1 hour of biodistribution (Figure 5A, left). After 24 hours of biodistribution, fluorescence was diffuse (Figure 5A, right), not only evident in the tumor region but also in other areas that could indicate biodistribution by the circulation of this type of nanomaterial (PMs). In order to know the real fluorescence-contribution of each tissue and organ, the *ex vivo* analyses were done in each time point (Figures 5B and 5C). In these studies, we could observe the typical intestinal and stomach fluorescence, due to the presence of chlorophyll contained in the feed-pellets, although the signal was significantly different to the control 1 hour after injection.

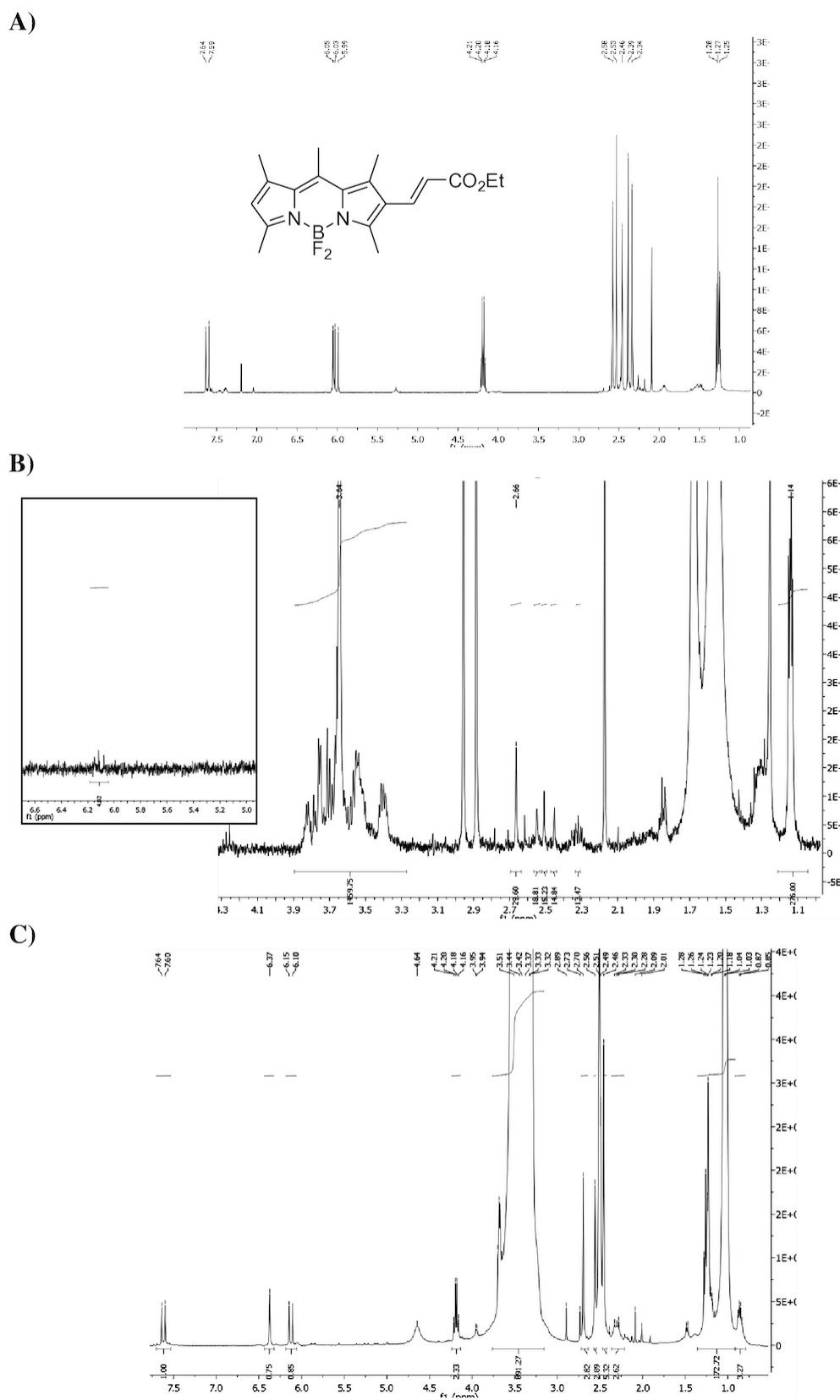


FIGURE 2 – Selected section of ^1H NMR spectra. **A)** For **BODIPY-ester**. **B)** For **T1307-BODIPY**. Inset: region of the H-pyrrole. **C)** For **L-T1307-BODIPY**. In **B)** and **C)** residual DMF was observed as doublet in the region near to 2.9 ppm.

Additionally, significant fluorescence accumulation in tumor and kidney tissue (not significantly different) by **L-T1307-BODIPY** was observed. Ex vivo studies,

24 hours after **L-T1307-BODIPY** injection, revealed no fluorescence differences in comparison with untreated animals (controls) (Figure 5C).

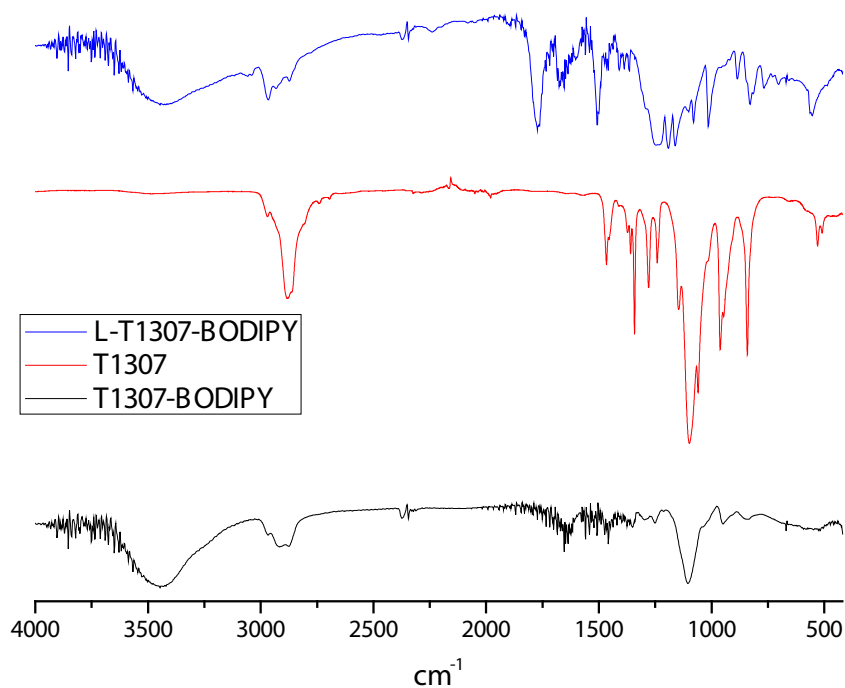


FIGURE 3 – FTIR spectra of **T1307** (red), **T1307-BODIPY** (black) and **L-T1307-BODIPY** (blue).

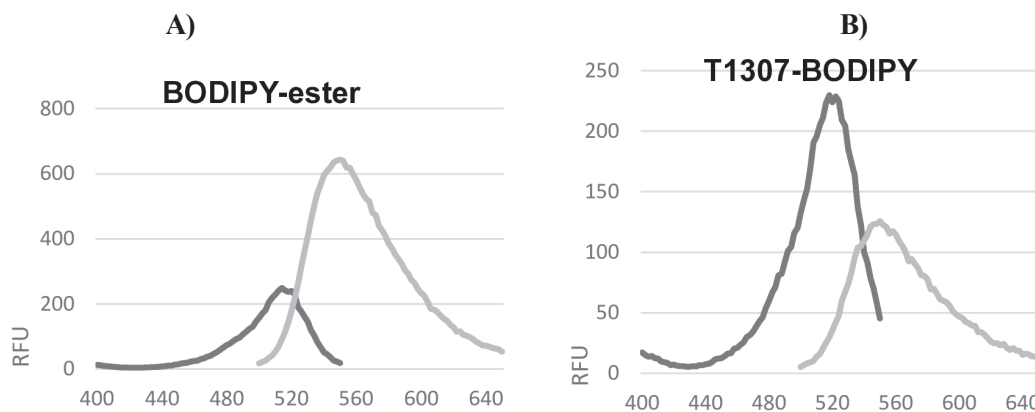


FIGURE 4 – UV/Vis absorption (black lines) and fluorescence excitation (gray lines) spectra. **A) BODIPY-ester** ($\lambda_{\text{emission}}$ (DMSO) = 550 nm). **B) T1307-BODIPY** ($\lambda_{\text{emission}}$ (PBS) = 550 nm) ($c = 1.0 \times 10^{-5}$ M, 20 °C).

Studies with radioactive probe-loaded T1307 PMs (L-T1307-^{99m}Tc)

^{99m}Tc loaded within T1307 PMs was successfully performed in a short time, producing good-yield L-T1307-^{99m}Tc. Afterwards, Microcon® centrifugation yielded the

desired probe with acceptable amounts of free ^{99m}TcO₄⁻ and ^{99m}TcO₂, according to the chromatographic studies, being the RP of 91.9 %, and without any negative effect on the properties of these PMs (aqueous solubilization, adequate pH and nanometric size).

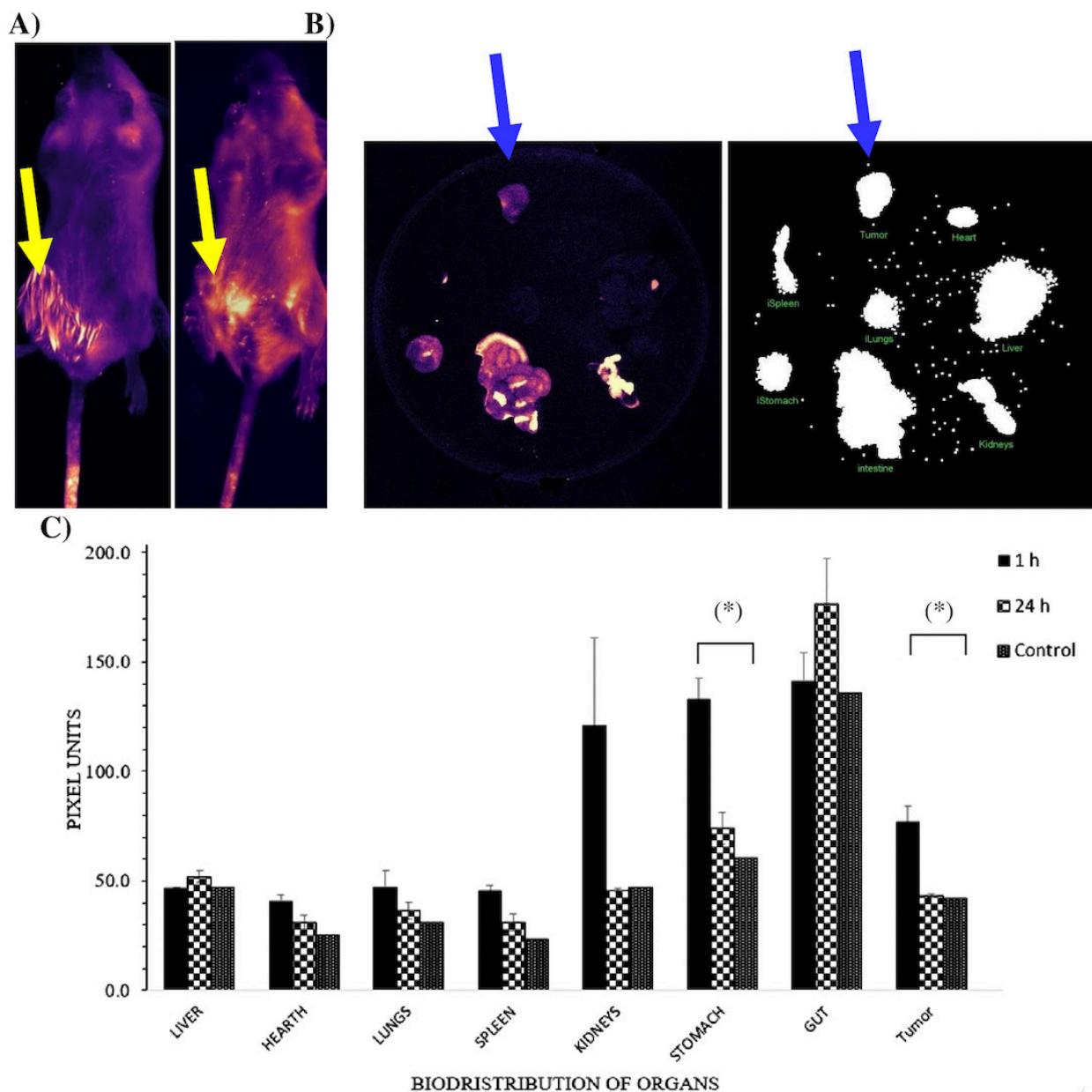


FIGURE 5 – A) *In vivo* images of Balb/c mice bearing 4T1 mammary tumor injected with L-T1307-BODIPY, 1 hour (left) and 24 hours (right) post-injections. Yellow arrows indicate the tumor location. **B)** Ex vivo images of organs, fluorescence mode (left) and X-ray (right) to calculate the maximum area of the organs, from Balb/c bearing 4T1 mammary tumor, 1 hour post intravenously injections of L-T1307-BODIPY. Blue arrows indicate the tumor. **C)** Fluorescence intensities in organs (in arbitrary units). (*) $p < 0.05$.

This radioactive probe was used to confirm the data obtained with **L-T1307-BODIPY**. After the IV injection of **L-T1307-^{99m}Tc**, mice did not reveal toxicity effects during *in vivo* studies according to the Irwin test (Dávila *et al.*, 2019). From the biodistribution studies, when **L-T1307-^{99m}Tc** was injected in the 4T1 breast tumor model developed in Balb/c mice, it was possible to observe the maximum radioactivity accumulations in the liver, the kidneys, the stomach and the tumor at 2

hours after the injection (Figure 6). As in the studies with **L-T1307-BODIPY**, the kidneys and the stomach were the organs with the main intensity 2 hours after the injection, with depuration occurring 4 hours post-injection. Tumor radioactivity remained almost constant between 2 and 4 hours with a slight decrease after 24 hours. The data indicated that **L-T1307-^{99m}Tc** in the studied organs could be observed up to 24 hours after the injection, correlated with the biodistribution of **L-T1307-BODIPY**.

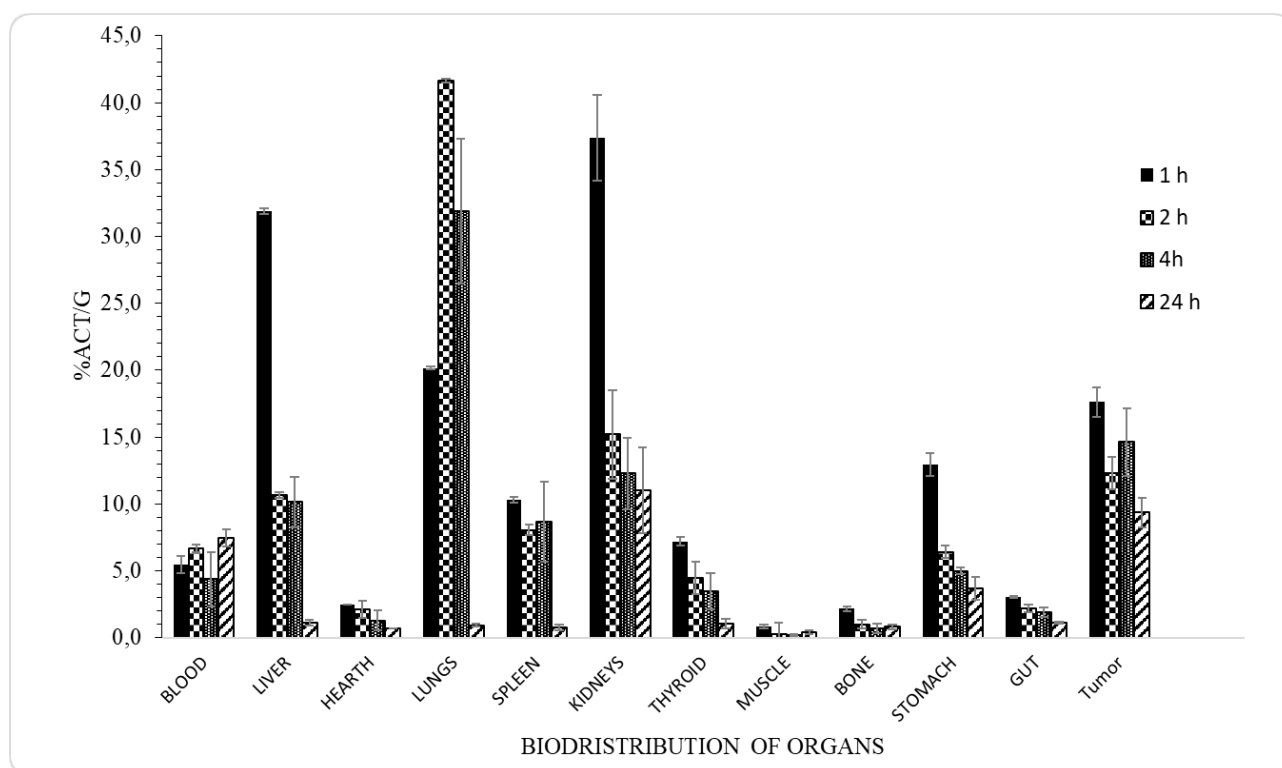


FIGURE 6 – Biodistribution of **L-T1307-^{99m}Tc** with time post-injection Balb/c with an induced 4T1 tumor at 1, 2, 4 and 24 h post IV injection.

CONCLUSIONS

The described probes in this work, based of X-shaped T1307 polymeric micelles loaded with BODIPY-derivative or ^{99m}Tc-radionuclide, showed a promising use for breast cancer imaging.

Further studies, employing other fluorophores with emission ranges close to the near infrared window, other radionuclides and other tumoral models are currently being performed.

ACKNOWLEDGMENTS

NL thanks ANII (Uruguay) and CSIC-UdelaR (Uruguay) for the financial support for doctoral studies (POS_FCE_2015_1_1005193). RJG is staff member of CONICET (Argentina). PC and HC are SNI-ANII (Uruguay) researchers. We thank ANII – Uruguay (FCE_1_2014_1_104714).

REFERENCES

- Acharya G, Mitra AK, Cholkar K. Nanosystems for diagnostic imaging, biodetectors, and biosensors. In: Mitra A, Cholkar K, Mandal A, editors. *Emerging nanotechnologies for diagnostics. Drug Delivery and Medical Devices*. Amsterdam: Elsevier, 2017, p. 217-248.
- Araujo L, Sheppard M, Löbenberg R, Kreuter J. Uptake of PMMA nanoparticles from the gastrointestinal tract after oral administration to rats: modification of the body distribution after suspension in surfactant solutions and in oil vehicles. *Int J Pharm*. 1999;176(2):209-224.
- Calzada V, Moreno M, Newton J, González J, Fernández M, Gambini JP, et al. Development of new PTK7-targeting aptamer-fluorescent and -radiolabelled probes for evaluation as molecular imaging agents: Lymphoma and melanoma *in vivo* proof of concept. *Bioorg Med Chem*. 2017;25(3):1163-1171.
- Chiang PC, Gould S, Nannini M, Qin A, Deng Y, Arrazate A, et al. Nanosuspension delivery of paclitaxel to xenograft mice can alter drug disposition and anti-tumor activity. *Nanoscale Res Lett*. 2014;9(1):156.
- Chiappetta DA, Sosnik A. Poly(ethylene oxide)-poly(propylene oxide) block copolymer micelles as drug delivery agents: Improved hydrosolubility, stability and bioavailability of drugs. *Eur J Pharm Biopharm*. 2007;66(3):303-317.
- Cohn D, Sosnik A, Levy A. Improved reverse thermo-responsive polymeric systems. *Biomaterials*. 2003;24(21):3707-3714.
- Cuestas ML, Glisoni RJ, Mathet V, Sosnik A. Lactosylated-poly(ethylene oxide)-poly(propylene oxide) block copolymers for potential active drug targeting: Synthesis and physicochemical and self-aggregation characterization. *J Nanopart Res*. 2013;15(1):1-21.
- Dávila B, Sánchez C, Fernández M, Cerecetto H, Lecot N, Cabral P, et al. Selective hypoxia-cytotoxin 7-fluoro-2-aminophenazine 5,10-dioxide: toward “candidate-to-drug” stage in the drug-development pipeline. *ChemistrySelect*. 2019;4:9396-9402.
- Eawsakul K, Chinavinijkul P, Saeeng R, Chairoungdua A, Tuchinda P, Nasongkla N. Preparation and characterizations of RSPP050-loaded polymeric micelles using poly(ethylene glycol)-b-poly(ϵ -caprolactone) and poly(ethylene glycol)-b-poly(D,L-lactide). *Chem Pharm Bul*. 2017;65(6):530-537.
- Fernández S, Berchesi A, Tejería E, Sanz I, Cerecetto H, González M, et al. Preparation and biological evaluation of (99m Tc)-labelled phenazine dioxides as potential tracers for hypoxia imaging. *Curr Radiopharm*. 2015;8(1):56-61.
- Gao JL, Shui YM, Jiang W, Huang EY, Shou QY, Ji X, et al. Hypoxia pathway and hypoxia-mediated extensive extramedullary hematopoiesis are involved in ursolic acid's anti-metastatic effect in 4T1 tumor bearing mice. *Oncotarget*. 2016;7(44):71802-71816.
- García MF, Gallazzi F, Junqueira MS, Fernández M, Camacho X, Mororó JDS, et al. Synthesis of hydrophilic HYNIC-[1,2,4,5]tetrazine conjugates and their use in antibody pretargeting with 99m Tc. *Org Biomol Chem*. 2018;16(29):5275-5285.
- Giglio J, Patsis G, Pirmettis I, Papadopoulos M, Raptopoulou C, Pelecanou M, et al. Preparation and characterization of technetium and rhenium tricarbonyl complexes bearing the 4-nitrobenzyl moiety as potential bioreductive diagnostic radiopharmaceuticals. *In vitro* and *in vivo* studies. *Eur J Med Chem*. 2008;43(4):741-748.
- Glisoni RJ, Chiappetta DA, Moglioni AG, Sosnik A. Novel 1-indanone thiosemicarbazone antiviral candidates: Aqueous solubilization and physical stabilization by means of cyclodextrins. *Pharm Res*. 2012;29(3):739-755.
- Glisoni RJ, García-Fernández MJ, Pino M, Gutkind G, Moglioni AG, Alvarez-Lorenzo C, et al. β -Cyclodextrin hydrogels for the ocular release of antibacterial thiosemicarbazones. *Carbohydr Polym*. 2013;93(2):449-457.
- Glisoni RJ, Sosnik A. Encapsulation of the antimicrobial and immunomodulator agent nitazoxanide within polymeric micelles. *J Nanosci Nanotechnol*. 2014a;14(6):4670-4682.
- Glisoni RJ, Sosnik A. Novel poly(ethyleneoxide)-*b*-poly(propyleneoxide) copolymer-glucose conjugate by the microwave-assisted ring opening of a sugar lactone. *Macromol Biosci*. 2014b;14(11):1639-1651.
- González-López J, Álvarez-Lorenzo C, Taboada P, Sosnik A, Sandez-Macho I, Concheiro A. Self-associative behavior and drug-solubilizing ability of poloxamine (Tetronic) block copolymers. *Langmuir*. 2008;24(19):10688-10697.
- Jiao L, Yu C, Li J, Wang Z, Wu M, Hao E. Beta-formyl-BODIPYs from the Vilsmeier-Haack reaction. *J Org Chem*. 2009;74(19):7525-7528.
- Lv S, Mingqiang L, Zhaohui T, Wantong S, Hai S, Huaiyu L, et al. Doxorubicin-loaded amphiphilic polypeptide-based nanoparticles as an efficient drug delivery system for cancer therapy. *Acta Biomater*. 2013;9(12):9330-9342.
- Maeda H, Wu J, Sawa T, Matsumura Y, Hori K. Tumor vascular permeability and the EPR effect in macromolecular therapeutics: a review. *J Control Release*. 2000;65(1-2):271-284.
- Marques Grallert SR, De Oliveira Rangel-Yagui C, Mesquita Pasqualoto KF, Costa Tavares L. Polymeric micelles

and molecular modeling applied to the development of radiopharmaceuticals. *Braz J Pharm Sci.* 2012;48(1):1-16.

Mi P, Cabral H, Kokuryo D, Rafi M, Terada Y, Aoki I, et al. Gd-DTPA-loaded polymer-metal complex micelles with high relaxivity for MR cancer imaging. *Biomaterials.* 2013;34(2):492-500.

Moghimi SM, Hunter AC. Poloxamers and poloxamines in nanoparticle engineering and experimental medicine. *Trends Biotechnol.* 2000;18(10):412-420.

Nardecchia S, Sánchez-Moreno P, de Vicente J, Marchal JA, Boulaiz H. Clinical trials of thermosensitive nanomaterials: An overview. *Nanomaterials.* 2019;9(2):E191.

Oda CMR, Fernandes RS, de Araújo Lopes SC, Oliveira MC, Cardoso VN, Santos DM, et al. Synthesis, characterization and radiolabeling of polymeric nano-micelles as a platform for tumor delivering. *Biomed Pharmacother.* 2017;89:268-275.

Rodríguez G, Nargoli J, López A, Moyna G, Álvarez G, Fernández M, et al. Synthesis and *in vivo* proof of concept of a BODIPY-based fluorescent probe as a tracer for biodistribution studies of a new anti-Chagas agent. *RSC Adv.* 2017;7(13):7983-7989.

Töster SD, Müller U, Kreuter J. Modification of the body distribution of poly(methylmethacrylate) nanoparticles in rats by coating with surfactants. *Int J Pharm.* 1990;61(1-2):85-100.

Wube AA, Hufner A, Thomaschitz C, Blunder M, Kollroser M, Bauer R, et al. Design, synthesis and antimycobacterial activities of 1-methyl-2-alkenyl-4(1*H*)-quinolones. *Bioorg Med Chem.* 2011;19(1):567-579.

Received for publication on 19th December 2019

Accepted for publication on 03rd February 2020